IMPLEMENTATION OF SACRIFICIAL SUPPORT STRUCTURES FOR HYBRID MANUFACTURING OF THIN WALLS

A Dissertation
Presented to
The Academic Faculty

by

Derek Vaughan

In Partial Fulfillment
of the Requirements for the Degree
Master of Science in the
George W. Woodruff School of Mechanical Engineering

Georgia Institute of Technology
December 2020

IMPLEMENTATION OF SACRIFICIAL SUPPORT STRUCTURES FOR HYBRID MANUFACTURING OF THIN WALLS

Approved by:

Dr. Christopher Saldana, Advisor
School of Mechanical Engineering
Georgia Institute of Technology

Dr. Thomas Kurfess
School of Mechanical Engineering
Georgia Institute of Technology

Dr. Andrzej Nycz
School of Mechanical Engineering
University of Tennessee

Date Approved: December 1st, 2020

ACKNOWLEDGEMENTS

I would like to thank my advisor Dr. Christopher Saldana for his guidance, feedback, and assistance throughout my time here at Georgia Tech. I would also like to thank Dr. Kurfess and Dr. Nycz for their time as my committee members, as well as my lab mates for working together with me and for providing assistance in my work along the way. Finally, to my Mom and Dad, I would never have been able to make it here without your constant support, thank you.

TABLE OF CONTENTS

LIST OF TABLES

LIST OF FIGURES

SUMMARY

Hybrid manufacturing enables a single machine to achieve the benefits of additive and subtractive manufacturing methods, allowing complex parts to be produced with less waste material and tight tolerances. One example of parts that have the potential to benefit from the use of hybrid manufacturing are those with thin walled features. Cutting forces can induce deflection in thin walls, which results in geometric error on the final part. Traditional thin wall machining uses the stiffer stock material to limit deflection by only machining at the current base of the wall. With hybrid manufacturing the feature is already near net shape prior to machining. This makes the production of thin walls more difficult as there is very little "stock" material to provide stiffness during machining. This work attempts to solve this problem by integrating sacrificial support structures to additively produced thin walls to increase their stiffness during machining. The supports are machined away while machining the thin wall itself. The angle, spacing, and height of these supports are varied in several experiments to observe the resulting geometric error and surface finish of these thin walls after machining. A comparison of time versus quality is then produced to determine the efficiency of changing the parameters of these support structures. The addition of these supports relative to the unsupported case provided a deflection reduction of around 0.2mm. Surface roughness is improved by approximately 1.5μm. Increasing values of support height correspond to reduced wall deflection. Similarly, decreasing values of support angle and support spacing improved geometric accuracy. Efficiency comparisons show that increases in print time correspond to rapidly diminishing gains in geometric accuracy but can continue to improve surface roughness.

CHAPTER 1. INTRODUCTION

Hybrid manufacturing is the combination of additive processes such as 3D printing and subtractive processes such as milling within a single machine. Hybrid manufacturing offers the potential to produce parts with increased complexity and lower waste material while maintaining a high level of dimensional accuracy. The machining of additively produced parts is often unchanged from methods used on cast or forged components. However, thin walled features present a challenge for hybrid manufacturing. Thin walls are often difficult to accurately machine due to large workpiece deflection from thrust and cutting forces applied during machining. Thin walled features often refer to features with an aspect ratio of height to width greater than 10:1. These features are relatively weak in their transverse direction, but usually maintain strength longitudinally making thin walls a lightweight method of improving the rigidity of a structure in specific directions. Thin walls are most commonly used as ribs for maintaining the stiffness of otherwise hollow shapes but could also consist of compressor blades or other thin shapes. An example of thin walls used in a ribbed structure is shown in Figure 1 below.

Figure 1: Aerospace component with machined thin wall ribs [21].

The problems that occur when machining thin walls are well-known and studied in the field of manufacturing. As the aspect ratio of a feature increases the deflection experienced on the wall increases exponentially. For a simple beam with a point load the deflection will be increase as $\delta \propto H^3$ where H is the height of the wall. The thrust and cutting forces produced by an endmill during the machining process can cause deflections high enough to create significant geometric error in the finished part. In addition to the large deflections that can occur during thin wall machining, the low stiffness of the feature also allows the part to be easily excited into chattering which results in a poor surface finish and additional geometric error. Traditionally, this would be offset by maintaining as much stock material as possible on the feature using a "step-down" approach [6]. Assuming the thin wall is being machined from a larger block of stock material, the unmachined portion of the wall is used to provide stiffness during material removal. One "step" of one side of the wall is both roughed and finished before the opposite side of the wall is roughed and finished. The toolpath then proceeds down to the next step of the wall. This process reduces deflection by only machining the stiffest part of the wall at each step. Reduced shank tooling is also used to prevent rubbing on previous steps of the wall [7].

However, for hybrid manufacturing this method is counterintuitive to implement. The near net shape features produced using additive manufacturing do not provide the excess structural support to implement the step-down method. Printing the feature much thicker than the desired shape would solve this but would also negate the material savings benefits offered by additive and would likely greatly increase the deposition time required for a given component.

Several works have focused on correcting for workpiece deflection through the use of simulation and trajectory corrections [29-31]. Path compensation can be used to correct for geometric error but still allows for the thin feature to chatter resulting in a poor surface finish. Path correction also requires complex models to calculate new trajectories that are unique to each workpiece. Physical fixtures have the potential to solve both deflection and chatter but are part specific and add additional steps to the manufacturing process. Instead, the use of sacrificial structures incorporated into the additive process to increase the stiffness of thin walled features should enable these features to be machined with higher geometric accuracy and lower surface roughness without greatly reducing the waste material reduction offered by hybrid manufacturing.

1.1 Problem Statement

With the demand for thin walled features in industry in combination with the growing adoption of hybrid manufacturing, the need for a method to produce high quality thin walls from near-net shape additive components is clear. No clear methods currently exist that address the problems of thin wall machining from the aspect of additive or hybrid manufacturing. The goal of the following work is to quantify the benefits of adding sacrificial support structures to improve the rigidity of printed thin walls during machining and to experimentally explore the design parameters of these sacrificial support structures. The angle, height and spacing of these supports will be varied to gain an understanding of how these features can best be utilized to support hybrid manufacturing.

1.2 Thesis organization

This thesis will start with an introduction covering a high-level overview of hybrid manufacturing systems and the problems that are faced when producing thin walls. Next, Chapter 2 will review research works related to the additive manufacturing and machining of thin features as well as cover the current state of blown powder direct energy deposition systems. Chapter 3 will cover the methodology used for the experiments performed in this thesis with a focus on the machining and additive parameters used. The results of the experiments performed will be presented and discussed in Chapter 4. Finally, Chapter 5 will summarize the major findings and contributions of the work and review potential limitations.

CHAPTER 2. BACKGROUND

This section will review existing technologies and research work that is related to hybrid manufacturing and thin wall machining. The first section will briefly review details of metal hybrid manufacturing as a whole and the general motivation behind the use of hybrid manufacturing systems. Next, the chapter will focus on powder based directed energy deposition technology as it is the system used for the work in this thesis. The second section of this chapter will look at the problem of machining high aspect ratio thin walls and a selection of published research into the problems related to machining thin walls using a variety of different techniques.

2.1 Overview of Hybrid Manufacturing using DED

2.1.1 Hybrid Manufacturing

Although the term hybrid manufacturing can reference a wide variety of different combinations of additive and subtractive processes, the majority of systems use CNC milling as the subtractive side and either wire-arc, wire-laser or blown powder additive manufacturing. Wire-arc systems utilize a spool of wire as the feed material that is then fed through a positively charged contact tip perpendicular to the base material and used to complete a high current circuit through the grounded base material. The high current melts the feed wire and allows for a molten metal deposition. An inert gas is injected around the melt pool to prevent oxidation of the deposited material. These systems are usually based on readily available metal inert gas welding equipment. Wire-arc additive offers high depositions rates around 10 kg/h [1, 2] at the cost of relatively low feature resolution of the

as-printed component. A typical wire arc melt pool will be around 8mm in width. Wire-laser systems use a similar system to wire-arc systems, but instead of using the wire as an electrode to produce an arc, a laser head is used to melt the wire as it approaches the base material. The use of a laser allows for finer control over the melting process, but also results in the loss of non-directionality that the wire-arc system provides as the wire feed stock must be mounted offset from the laser head. Changes in wire feed angle into the laser focal point can then result in varying print characteristics.

Blown powder additive manufacturing will be the additive process used in this work. Blown powder additive uses a laser head as the energy source for melting the feed material, but replaces the wire feedstock with metal powder.

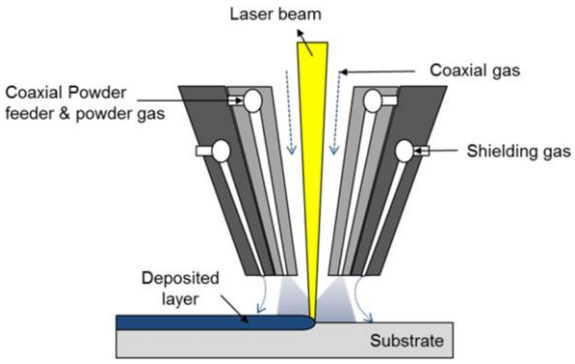

Figure 2: Blown powder deposition nozzle [3]

As shown in Figure 2, the metal powder is fed coaxially around the laser head along with shielding gas and a second inert gas flow that is used to transport the metal powder to the nozzle. Initially the metal powder is stored in hoppers where a gravity fed metering disc is used to supply the designated amount of powder into a small tube where an inert gas flow is used to transport the powder to the deposition head. The laser is focused to a designed nozzle offset to ensure sufficient power is applied to the metal powder to liquify

the material as well as obtain a spot size large enough to fully encompass the powder flow. The benefits of this system are relatively fine controllability of input parameters and print resolutions where beads widths are around 1mm typically at the cost of lower deposition rates, although they can range from 1 g/min to 15 kg/h for specialized systems [4, 5].

Additive manufacturing offers a high degree of flexibility in design with the ability to produce geometries such as internal channels, lattices, and overhangs that would otherwise be difficult or impossible to produce using other manufacturing methods. The surface finish of the printed parts can vary and depends on the process and parameters used. Laser powder bed fusion systems can produce parts with Ra values ranging from 8μm to 40μm [8, 9]. Meanwhile wire arc systems can have surface roughness on the order of 0.1mm or higher [10]. These rough surface finishes can be problematic for any features that need to interface with an assembly and additional post processing steps for printed components. Hybrid manufacturing streamlines this process by enabling post process milling to be performed in the same machine. This also allows for the coordinate system used during the additive process to be reused for machining. Without hybrid manufacturing it can be difficult to align a printed part to a coordinate system due to the large print resolution [11]. Hybrid manufacturing also benefits from the material savings provided by additive manufacturing. Thin walled structures in particular have the potential to benefit greatly from hybrid manufacturing. In aerospace components there can be a 30:1 ratio of material purchased to material used in the final part [6].

There are several commercially available systems for hybrid manufacturing. The Mazak AM series offers 5-axis and mill turn machines with blown powder and wire laser additive capabilities [12]. These systems utilize printing heads mounted offset from the

machining spindle that then extend to operate coaxially with the spindle or operate from a specified offset location. DMG Mori offers a similar system with their Lasertec 65 DED hybrid system on a head that extends to operate coaxially in front of the spindle head [13]. Hybrid Manufacturing Technologies offers blown powder processing heads to be installed directly in CNC tool holders and magazines [14]. This enables the ability to retrofit additive capabilities onto an existing machine tool.

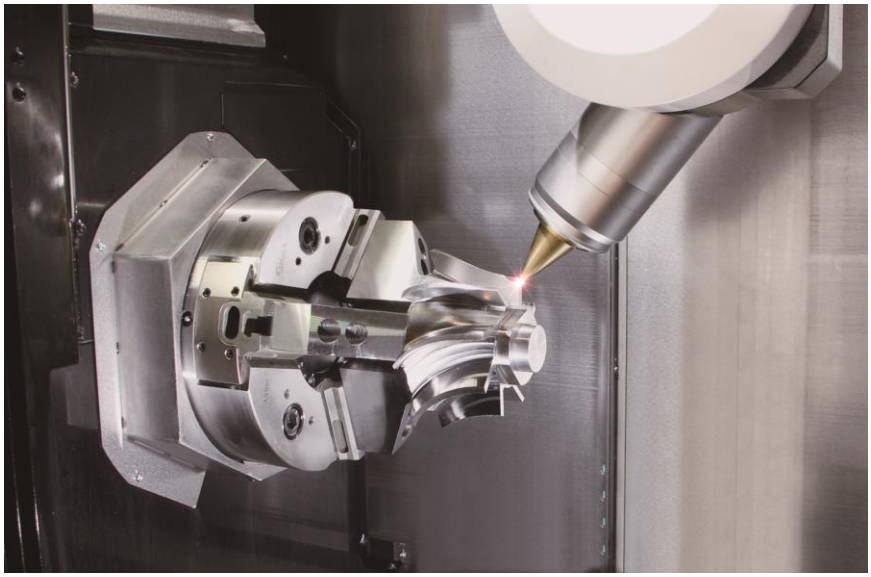

Figure 3: Mazak INTEGREX i-400AM using blown powder additive head for blade repair

The MPA 40 by Hermle is another 5-axis hybrid machine with an offset print head, however this system uses a kinetic thermal spray process for the additive side instead of a laser as an energy input [15]. This system has the ability to print dissimilar materials or water-soluble filler materials due to the deposition material being micro-forged to the base material rather than melted and fused.

2.1.2 Directed Energy Deposition

DED systems cover a variety of different additive manufacturing processes. Different DED processes will have varying deposition rates, print resolutions and geometric capabilities. In general, systems with a higher deposition rate like wire-arc deposition will have conversely poorer print resolutions. Laser DED systems are roughly in the middle of the spectrum for deposition rate and resolution. Laser powder DED systems are most commonly used for hybrid manufacturing, although laser wire and wire arc systems are also used. Powder bed systems are not used as often in hybrid applications due to the need for a controlled environment for electron beam energy sources and powder spreading which increases system costs. Commercial powder bed systems such as the Matsuura LUMEX Avance-25 are available however [20]. Laser DED systems use a fiber laser with optics mounted to the print head to direct energy into the feed material. The power of this laser can range from 100W to several kW [16]. Increasing power enables increased deposition rates at higher laser and operating costs. Higher deposition rate systems such as wire arc require a much higher heat input which can make thin features difficult to maintain thermally. The power level of laser systems can be digitally controlled which enables precise control of the heat input into the process. The ability to control the heat input into the printing process is important due to its impact on the microstructure and mechanical properties of the completed part [17-19].

2.2 Overview of Thin Wall Machining

The problems that occur during thin wall machining have been noted and researched for some time [7, 22, 23]. There are two primary problems when machining thin walls, both of these problems are caused or extenuated by the low stiffness of the feature. The first problem is self-excited vibrations between the cutting tool and workpiece known as chatter. Chatter typically occurs when the stiffness of the tool is insufficient to prevent bending due to a long stick-out or excessive cutting forces. Chatter can also occur from a variety of other sources such as the spindle, fixturing, and part geometry. In the case of thin walls, the low stiffness of the wall itself results in high frequency vibrations that readily result in chatter regardless of tool stiffness [24]. This chatter leads to a poor surface finish on the machined wall and increases tool wear. The second problem when producing thin walls is the elastic deformation of the wall due to the machining forces required for material removal.

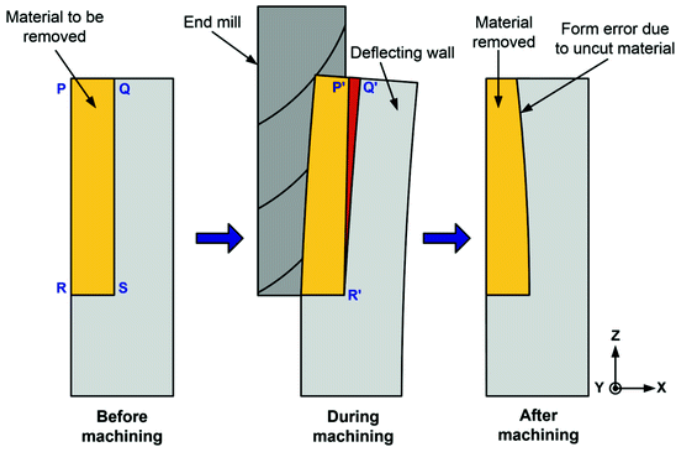

Figure 4: Illustration of how thin wall geometric error can occur from deflection due to machining forces [25].

In any machining process, some portion of the forces applied to the workpiece are perpendicular to the surface being machined. This force is known as the thrust force and can be calculated as:

$$F_{thrust} = F_{cutting} \tan(\beta - \alpha)$$

$$\beta = \tan^{-1} \mu$$

Where $F_{cutting}$ is the force applied parallel to the workpiece surface, β is the friction angle, α is the rake angle of the tool, and μ is the coefficient of friction. Assuming a coefficient of friction of 0.5 and a rake angle of 10° this would result in roughly 30% of the cutting force as the thrust force. With the rotation of the tool the cutting force component will also point roughly tangential to the workpiece surface at the start or end of each chip depending on milling direction. When these forces are applied to thin walls result in plastic deformation of the wall away from the tool. As shown in Figure 4, the wall will experience the highest deflection at the top of the wall which results in a feature that is wider at the top than the bottom. A variety of works have been completed to model the magnitudes of this deflection, but typically deflection typically ranges from 0.01mm to 0.1mm in size [26, 27].

2.2.1 Thin Wall Deflection Prediction

In order to prevent the deflection and chatter problems that arise when machining thin walls, a variety of different solutions have been proposed. This section will review past works that aim to solve the problem through parameters and tool path modifications. Wang et al, [28] uses an algorithm to build on typical step-down machining by optimizing

the material removal steps in order to maximize stiffness throughout the process. A block of the material to be removed is subdivided into sections by the algorithm to determine the stiffest material removal order. The experimental results showed significant reductions in deflection over the baseline step-down method. Koike et al, [29] used a similar method, however the orientation of the tool was also considered in the algorithm. Tool orientation was varied in order to direct the cutting force vector in the direction of highest stiffness on the part. This method took significant time to calculate but saw a roughly 10N reduction in cutting forces. However, these two methods rely on the use of the existing stock to maintain stiffness, which is not present in near-net shape hybrid components. Ratchev et al, [30] used finite element analysis to predict the deflection of a workpiece with a theoretical force model. Later, Ratchev et al, [31] used this model to implement modified tool paths to compensate for the geometric error produced due to wall deflection. Cutting points were taken along the tool path and correlated with the predicted FEA model deflection to generate modified cutting points to build the compensated tool path. Using this method, the thickness error was reduced by roughly 0.3 mm on an aluminium wall with a 24:1 height to width ratio. Ge et al, [34] bypassed the need for FEA modelling and used in-process probe measurements on thin webs after performing a semi-finishing pass to obtain geometric error. The error was then filtered and used to generate modified tool paths to correct for the error. These processes assist in the reduction of geometric error on thin walls but do not help to compensate for chatter which leaves the possibility of poor surface finishes. Budak et al, [32] used FEA to determine the frequency response function of a part during machining to attempt to avoid chatter. The FRF was determined initially and then modified based on the material removed from the part. The FRF was then used to create

stability lobe diagrams for parameter adjustment enabling small blades to be finished with relatively little chatter. Tang & Liu [33] used a three-dimensional version of the stability lobe diagram to find that a larger exit immersion angle correlated to an increased stable MRR for thin walls. The relatively constant bead width produced from additive manufacturing makes it difficult to significantly alter the cutting depths in hybrid manufacturing without printing excess material.

2.2.2 Thin Wall Fixturing

This section will review past works designed to prevent deflection and chatter of thin walls through the use of physical devices to improve the stiffness of the workpiece or to reduce potential sources of vibration in the process. Smith et al. [35] machined sacrificial structures during the roughing of thin walls to increases the stiffness of the walls during finishing passes. Several different support schemes were modelled using FEA to determine effectiveness. Two thin wall enclosures were then machined using this technique. FEA results from this work showed that with one sided buttress only roughly 50% of the material needed to be machined away. This concept served as the basis for the work performed later in this thesis.

Figure 5: Thin Walled Structure using machined sacrificial supports [35].

This work showed the potential to use sacrificial structures to minimize geometric error and surface finish but did not look at the specific details of the problem. Zeng et al. [36] developed a model taking into account workpiece vibrations to determine where fixtures should be located on a particular structure to dampen vibrations on thin walls. Each side of a square thin walled structure was split into 36 sections to establish which sections would require an external fixture to minimize vibrations during machining. Kolluru et al. [37] used a similar approach but used tuned masses and neoprene sheets attached at regular intervals to a thin walled cylinder to reduce milling vibrations. FEA and impact testing were used to determine appropriate masses to attach to the thin wall. In the machining experiment, vibrations were reduced 4.2 times compared to the neoprene sheet alone. Kolluru & Axinte [39] later found that the adhesive used for mounting the masses proved difficult to remove after machining. In response, a torsion-based fixture was created to push against the thin cylinder to improve stiffness. This was found to be easier to implement and improved upon the vibration reduction found with the previous method. In addition to these works, there are also existing methods for improving the rigidity of parts such as using wax

for fixturing the component [38]. The wax has a relatively low melting temperature and can be poured over the thin wall and the thin wall can then be machined normally. However, this requires a method of containing the wax around the thin wall and requires additional post processing to remove the remaining wax after machining. Additive byproducts such as spatter from wire-arc or unmelted powder from blown powder would likely contaminate the wax and limit reusability as well. Taking this concept further, Jiang et al. [40] used magnetorheological fluid in a magnetic field as a damping medium. The part was fixtured in a container and the fluid was poured around the part and solidified. Post process removal of the magnetorheological fluid would likely be easier than wax, but would remain necessary.

CHAPTER 3. METHODOLOGY

This section will cover the methods used to produce and evaluate the impact of sacrificial support. Laser DED parameters were explored with an emphasis on laser power and path planning to produce basic thin wall featured using hybrid manufacturing. Several different machining strategies and parameters were also tested to minimize the influence of chatter and provide reasonable support comparison results. The experiments were designed to be used as a baseline on the effect of different support geometries and implementations that could be extrapolated for use on more complex thin wall features.

Table 1: Experimental conditions tested for sacrificial support structures

Condition:	Unsupported	Sacrificial Supports						
Angle (α) (°)	-	45	65	85	65	65	65	65
Spacing (S) (mm)	30	30	30	30	10	50	30	30
Height (H) (mm)	-	30	30	30	30	30	10	20
Thickness (T) (mm)	0.5	0.5	0.5	0.5	0.5	0.5	0.5	0.5

Three different support parameters were studied and their impact on the quality of the resulting thin wall evaluated. These parameters relate to the sample geometry shown in Figure 6. The condition sets to be evaluated are shown in Table 1. The first parameter investigated was support angle (α). It is assumed for these experiments that a triangular support will be the most practical shape to apply as a support, however the angle of the triangle must be investigated. The second parameter to be varied is support height (H). A sufficiently short thin wall may have a low enough deflection such that supports are unnecessary. Similarly, if the sacrificial supports limit deflection enough, that they would not be needed for the full height of the wall. The third parameter was the spacing used

between each support (L). If only a single mode of deflection perpendicular to the thin wall is considered, theoretically only a single set of supports would be required for a given feature. However, the effect of torsion on a 3D wall requires a look at how the part will deflect when the spacing between supports is varied. All of these parameters ultimately correspond to a variation in print time and the final quality of the finished thin wall due to the resistance of machining forces.

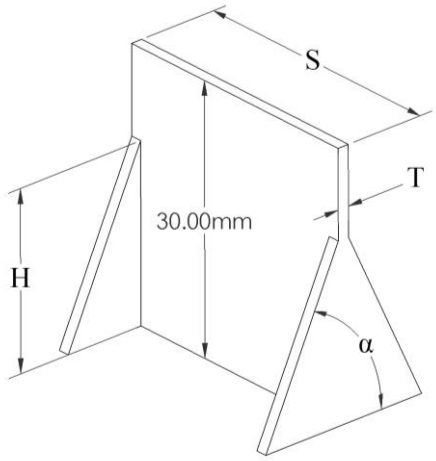

Figure 6: Illustration of the three parameters to be tested in the experiment with H representing the height of the support, S representing the distance between each support, T is the fixed thickness of the wall, and α representing the angle of the support measured from the horizontal

In order to test the impact of these three parameters on the quality of the machined thin wall, 24 samples were produced. Three unsupported walls were printed and machined to serve as the baseline for the experiment. These three samples were 30mm in length and 30mm in height. In the as-printed condition, the thin walls averaged at 1.46mm thick and were machined to an expected thickness of 0.5mm. This provided an aspect ratio of 60:1 which would readily produce typical problems expected with thin wall machining. A thickness of 0.5mm was chosen to ensure that a continuous surface was obtained after machining. If less material was removed, samples with high geometric error would be

found where the as-printed surface would still be visible near the top of the wall. Next, the impact of support angle was tested by producing thin walls with triangular supports with angles of 45, 65, and 85 degrees. The angle was measured between the hypotenuse of the right triangle and the build plate. Three samples were produced for each angle to account for potential error. Each sample remained 30mm in length and height. The next parameter test involved producing samples with varying support height. 65-degree triangular supports were implemented as before, but instead extended to 10mm, 20mm, and 30mm in height. The thin wall remained 30mm in height and length. Finally, the effect of support spacing was tested by producing samples with varying distance between each support. 65-degree supports that extended to the 30mm height of the wall were used, but the wall length was varied at 10mm, 30mm, and 50mm. All of the produced samples were then machined using identical parameters and tooling to produce a thin wall with an expected thickness of 0.5mm. The toolpaths for the additive and subtractive processes were produced using MATLAB. A sample additive path is shown below in Figure 7. The additive path alternated in direction to minimize asymmetry in the printing process, as described in section 3.1.1.2.

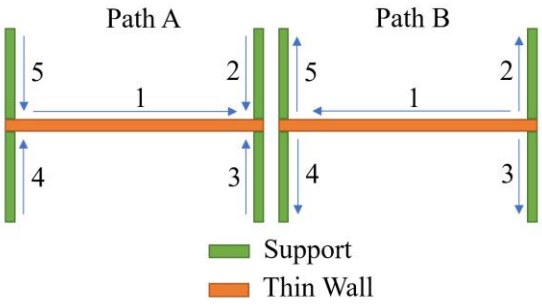

Figure 7: Additive toolpath used for producing supported thin walls showing how print paths alternated between Path A and Path B for each additive layer to avoid part asymmetry

After machining each sample, excess build plate material was cut away from the thin wall using a bandsaw. The surface roughness was collected using a contact profilometer and the geometry was measured using a coordinate measuring machine. Data was primarily collected near the top of the wall as the highest deflection was consistently found to occur at the top of the wall and can be assumed to be the worst-case scenario location for each sample.

3.1 Parameter Development for Producing Thin Walls

Parameter development is a necessary first step when working with a new material in hybrid DED processes. Variances in material density and melting temperature, as well as composition can alter how the material deposits when using the additive manufacturing. Additionally, thin walled features can also require parameters that differ from parameters used to produce more substantial parts. The energy required to allow for effective fusion between the blown powder and the base substrate or layer below it can also cause thin walled features to overheat. As the thin walled feature increases in temperature the laser can begin to fully melt previous deposition layers to a degree that may prevent the thin feature from properly forming. Conversely, if too little energy is used, the powder will not properly melt resulting in porosity and poor material characteristics. This is particularly an issue for the first few layers of a thin walled feature. For the first few layers the deposition location is very close to the much larger build plate and energy can quickly dissipate away from the melt pool which can lead to poor fusion between the thin walled feature and the base plate. Even if the base plate is not to be used for the final part, the low substrate temperatures can result in poor material characteristics for these layers.

3.1.1 Directed Energy Deposition Parameters

The machine used for production of the hybrid thin walls and sacrificial support structures was a Mazak VC-500AM. This machine is based on the Mazak VCU-500 5-axis machine in combination with a 1kW IPG Photonics fiber laser and Oerlikon powder hopper units for blown powder DED processes. The material used for the sacrificial support structure experiments was 316L stainless steel. Specifically, Carpenter Additive LPW-316-AAAW powder was used. The composition of this powder is shown in Table 2. This powder has a size distribution of 44-106 microns. This material was chosen primarily due to its availability and prior use on the VC-500AM. Although typical thin walls in fields such as aerospace are often made of aluminium or titanium, the sensitivity of changing geometric parameters of sacrificial support structures should readily transfer between materials while the scale of geometric error should be expected to vary.

Table 2: Additive powder chemical composition

	C	**Cr**	**Cu**	**Fe**	**Mn**	**Mo**	**N**	**Ni**	**O**	**P**	**S**	**Si**
Min wt%	0	17.5	0	Bal	0	2.25	0	12.5	0	0	0	0
Max wt%	0.03	18.0	0.5	Bal	2	2.5	0.1	13.0	0.1	0.025	0.01	0.75

3.1.1.1 Parameter Scans

Initial parameter tests to find effective additive deposition values were designed around prior user experience with the material and machine. Two parameter full factorial analysis was performed for laser power and print head feed rate. Laser power was varied between 175W and 250W in 25W increments and feed rate was adjusted between 160mm/min to 240mm/min in 10mm/min increments. The build plates used were 0.25”

hot rolled 304 stainless steel. Each plate was cleaned using isopropyl alcohol prior to the additive process.

Figure 8: Parameter sweep sample for 316L powder deposition testing 27 different parameter combinations

As shown in Figure 7, single track walls were printed for each combination of parameters. Each wall was roughly 1cm in height which equated to 30 printed layers to ensure the thin feature approached a steady state. After testing all parameters, the thin walls were found to be relatively insensitive to laser power and feed rate within the range of values tested. The lower range of laser powers tested were found to have poor build plate fusion with the thin wall. After cooling some thin walls were visibly separated from the build plate without any external forces being applied. To ensure effective build plate fusion, 275W was chosen for laser power for the first layer of each wall only. Parameters for the remaining layers in the build are shown in Table 3 and were chosen based on observations from the parameter sweep for parameters that appeared to produce consistent layer heights. The thin walls were found to be far more sensitive to the distance between the print nozzle and substrate. Due to the low surface area on the top of the wall, distances greater than 3mm were found to have poor powder catchment on the substrate resulting in very short layer heights. The poor powder catchment was also found to result in uneven layer heights.

Any external factors that may occasionally impact powder flow such as turbulence in the gas flow, or small clumps in the powder would result in a minor change in layer height. With the poor powder catchment any minor underbuilding would continue to be exaggerated by the small increase in distance between the print nozzle and substrate and ultimately result in a major defect in the print. To solve this issue the print nozzle was set to stay within 3mm of the substrate where powder catchment was found to remain relatively consistent and was even noted to self-level in some cases.

Table 3: Laser-Powder DED Machine Parameters

Laser Power (W)	Nozzle Gas (LPM)	Shielding Gas (LPM)	Disk Speed (%)	Carrier Gas (LPM)	Feed Rate (mm/min)
225	2	6	35	6	160

Bead-to-bead spacing was also tested prior to running the experiments to ensure that the sacrificial supports were properly fused to the thin wall during printing. Bead-to-bead spacing refers to the distance between two beads that make up a single feature within a layer. In particular, the distance between the beads in each support and the beads that composed the wall were varied. The thin walls produced during the parameter sweep were measured to have an average as-printed thickness of 1.46mm. Based on this measurement, initial samples were printed with a distance of 1.46mm between the center of each bead. These samples were found to overbuild in locations where two beads met within a layer. The contact point between two beads likely experiences improved powder catchment resulting in a larger than expected bead width at the point of intersection. At a bead-to-bead spacing of 1.6mm, insufficient fusion between the support structure and the thin wall was found. This resulted in the sacrificial supports disconnecting from the thin wall during machining. A bead-to-bead distance of 1.5mm was determined to provide acceptably low

overbuilding at bead intersections while also providing sufficient fusion to the thin wall to remain connected to the thin wall during machining.

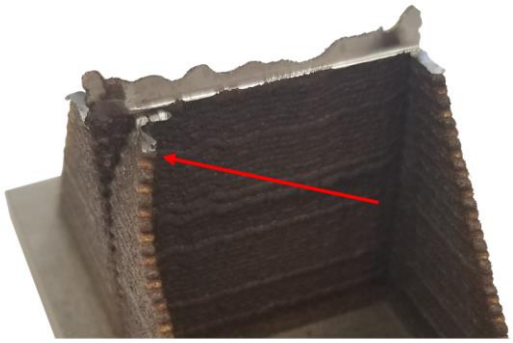

Figure 9: Example of poor bead-to-bead fusion support failure indicated by red arrow; caused by excess bead distance between thin wall and support

3.1.1.2 Starts and Stops

In the first parameter sweep print, the walls were printed with the start and stop position for the additive head in the same position for each layer. This was found to cause the walls to grow much more quickly at the start position than the remaining section of the wall which produced a significant defect within 15 layers. The problem of overbuilding at the beginning of each bead was found to be due a delay in the laser power during deposition. The machine paused at the start of each bead and waited for the laser to turn on before beginning to feed along the specified path. This delay caused the start of the print path to overbuild. For the second print, the start and stop positions were swapped after each layer to minimize this overbuilding. Alternating start points appeared to largely eliminate the overbuilding due to machine lag. Taller thin walls were also found to underbuild on both ends with alternating start points. This suggests that the machine can more quickly turns off the laser at the end of each bead than it is able to activate the laser at the beginning of the bead. To compensate for this, a G4 dwell was used to pause for 0.1 seconds at the

end of each bead. The use of alternating bead paths and dwells at the end of each bead was found to produce consistently even layer heights as long as the print head remained within 5mm of the substrate.

3.1.2 Machining Paths and Parameters

Each of the 24 samples were machined using the same toolpath to ensure a reasonable comparison between changes in support structure variables. All samples were machined using the same VC-500AM machine that was used to print the samples. The machining parameters used were intended to provide typical quality and were not extensively optimized to improve machining time or part quality. Traditional methods of finishing thin walls were used to provide practical results. Due to the relatively small scale of deflection being measured, attempts to reduce deflection through the machining path would have obscured changes between parameters in the sacrificial supports. However, some parameter optimization was required to ensure the thin wall and sacrificial support structures did not fail during the machining process.

Samples were machined using a modified step-down approach where the support structure for a given step was machined away before machining the thin wall. The opposite side of the wall was than machined using the same process. Due to the relatively small amount of material to be removed from the thin wall only a single rough/finish pass was used for each step. Down milling was used for all machining paths, however up milling was also tested and appeared to provide similar results. The support structures were machined along a path parallel to the support itself with the tool slightly offset from the support. Initial sample machining paths where the tool followed a path colinear with the

support structure failed due to the support structure bending over during machining. This was likely due to the cutting forces applied directly perpendicular to the support itself. Offsetting the toolpath to the side of the support allowed the cutting forces to be applied in a direction of higher strength for the support and prevented support failure. Figure 10 below shows the steps followed during the machining of two steps during the machining process.

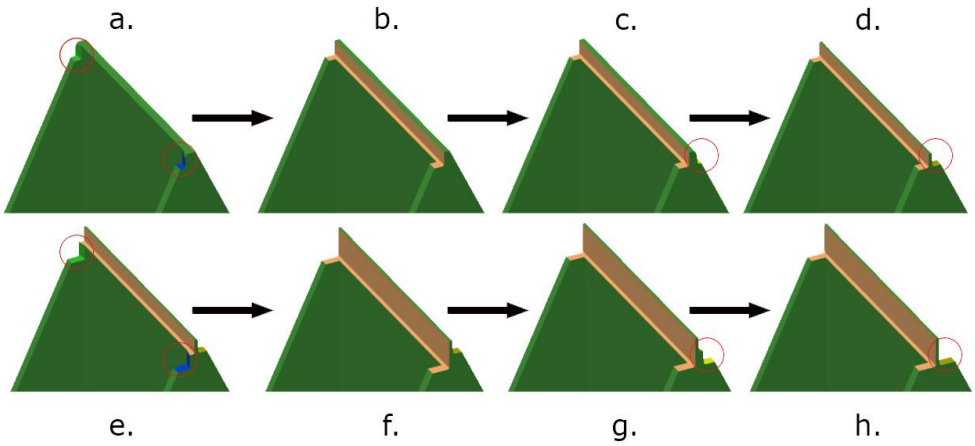

Figure 10: Machining process for thin walls: a) sections of supports are removed. b) section of wall is machined. c) sections of supports on opposing side of wall are removed. d) section of wall is machined on opposing side of wall. e-h) Process repeats for next step down, red circles indicate support removal locations.

Prior to machining the face of each thin wall, the support material for a given step was machined away to attempt to minimize an increase in radial depth of cut while machining the face of the thin wall. This process is shown in step a, c, e, and g of Figure 10. The radial depth of cut (R_d) still increased by approximately 1mm when milling the wall face at locations coincident with the support structures and resulted in different surface finishes and geometry at the edges of each sample. No measurements were taken from the edges of any of the samples to account for this potential source of error. The ends and top surface were not machined as these surfaces were not the focus of this experiment. Several initial test samples were machined on the top face of the wall and this was found to cause

significant deflection for the unsupported case and resulted in plastic deformation for unsupported thin walls, therefore it was not machined to avoid adding additional confounding factors to the experiment.

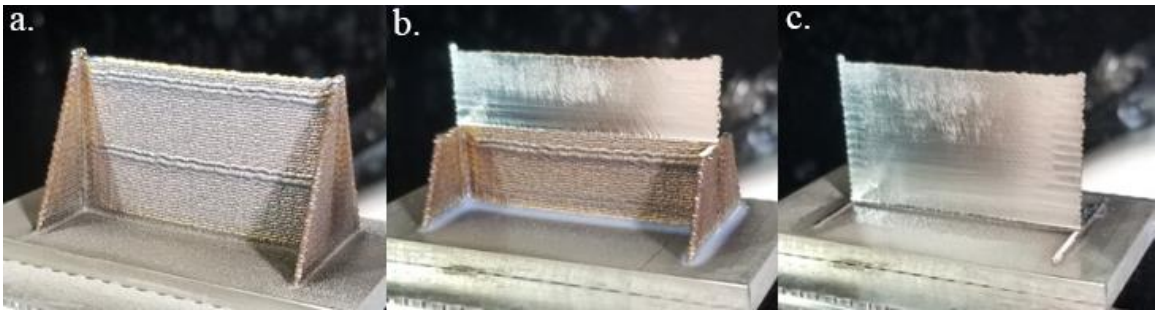

Figure 11: Supported wall [α=65°, H=30mm, S=50mm] showing: a) as printed. b) halfway through machining. c) after machining

Figure 11 shows the 50mm wall length sample before, during, and after machining. Figure 11(a) shows the as-printed thin wall with attached sacrificial support structures. Overbuilding from the additive process can be seen at the top of each support structure. Several deposition layers seen roughly halfway up the wall and near the top of the wall are also thicker than other layers. This was done manually during the printing process to assist in minimizing overbuilding during deposition. Figure 11(b) shows the same wall partially machined. Chatter can be observed near the center of the wall, and is less prevalent near the support structures on the wall. Figure 11(c) shows the fully machined thin wall. Surface finish can be seen to improve significantly halfway down the wall. It can also be noted that the surface finish at the top left of the wall changes between Figure 11(b) and Figure 11(c). This change is due to tool rubbing after the initial machining pass at the top of the wall and will be addressed in the results.

3.1.2.1 Machining Parameters and Tooling

Tooling for machining each sample was chosen to attempt to minimize potential extraneous effects that could alter the final results. Preliminary tests used a 0.125" ball end mill. With a 4mm step down (A_d), the thin walls produced were found to be significantly oversized at their base. This was likely due to a large level of tool deflection from machining forces. To ensure that tool deflection was negligible when measuring the final part geometry, the step-down distance was reduced to A_d=2mm to reduce cutting forces. A larger diameter straight end mill was also chosen to further eliminate any possible tool deflection. Based on recommendations from Kennametal, the tool chosen was a 0.5" 5-flute end mill. 5 flutes were chosen to avoid potential hammering effects from a lower flute count and to avoid high radial pressure from a high flute count which could increase the potential for chatter. The end mill also has variable flute pitch to further help prevent chatter. The end mill was mounted in a shrink fit tool holder to minimize any potential runout. The tool stick-out was set at 40mm to allow for 10mm of additional space between the thin wall and tool holder in the event of overbuilding during the additive process.

Table 4: Machining Parameters for Thin Wall Samples

Tool Dia. (mm)	Flute Count	Speed (s) (RPM)	Feed (f) (mm/min)	Axial Depth of Cut (A_d) (mm)	Radial Depth of Cut (R_d) (mm)
12.7	5	1720	200	2	0.475

Table 4 shows the feed and speed used for machining the sacrificial support structures and the thin wall itself. These parameters correspond to approximately 0.001 inches per tooth. These parameters were chosen to attempt to minimize the effect of chatter on the final results. In practice, a higher feed rate would likely be desirable but would

potentially require additional experimentation or stability lobe analysis to determine appropriate parameters.

3.2 Geometric Error – Coordinate Measuring Machine

Geometric results for all samples were obtained using a Zeiss Micura coordinate measuring machine (CMM). This machine provides accuracy to within 0.7 µm plus cosine error. Preliminary measurements using a micrometer served to prove that this accuracy would be sufficient for the expected changes in part geometry. Preliminary scanning paths used a single probe oriented downward towards the build plate. During scanning this probe was found to collide with the thin wall along its shaft rather than the rounded tip. This was most likely due to the use of a bandsaw to separate the samples from the excess build plate which resulted in a non-perpendicular geometry on the sides of the remaining build plate. This required the samples to be scanned using two probes mounted horizontally to avoid unintended collisions as shown in Figure 12. Initial scan paths attempted to quantify the perpendicularity of the wall relative to the build plate but found the raw build plate surface coupled with stray powder deposition resulted in inconsistent results. The two probes used for measurement were recalibrated directly prior to collecting data to ensure minimal measurement error. Temperature compensation was also used based on a single temperature sensor mounted to the vice used for sample holding with a coefficient of 17e-6 $\frac{\mathrm{m}}{\mathrm{m°C}}$.

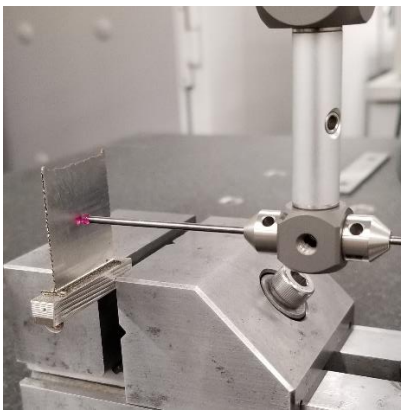

Figure 12: Coordinate Measuring Machine Probe During Scanning.

The thickness of each sample was measured in 6 different locations as shown in Figure 13. Each location was represented by a 2mm by 3mm patches on each side of the wall with 12 total patches. All patches were 2mm away from nearby edges to avoid effects from the larger radial depth of cut (R_d) experiences when machining across sections of the wall with leftover support material. The perimeter of each patch was scanned using the CMM to fit a plane to each location. The plane was created using least square fitting to minimize influence from chatter on geometric results. The distance between two patches on opposite sides of the thin wall was then calculated from the center of each patch and parallel to the line that most closely approximates the perpendicular between the two planes. This method ensures that if the wall was not mounted perfectly perpendicular in the vice the thickness measured would not be influenced. The flatness and perpendicularity of each side of the wall relative to a datum “B” was also measured using a scanning path that encompasses the entire surface of the wall.

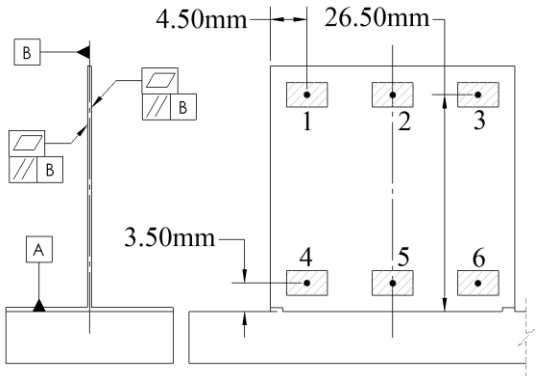

Figure 13: Drawing showing CMM patch scan locations 1 through 6 for measuring thickness, and datum locations for part orientation

When scanning a sample using the CMM, a fixed amount of force was applied on the sample from the probe. Due to the low stiffness of the samples, this could represent a significant deflection during scanning and result in measurement error for the samples. To quantify this error, a dial indicator was used to observe the deflection of a 30mm sample during a probe scanning routine. A deflection of 0.0076mm was observed at a height of 23mm. Based on a simple beam deflection this would correspond to a deflection of 0.0117mm at the height thickness was collected from. Assuming this error compounds when measuring both sides the measured thickness can be expected to be 0.0234mm smaller than the real thickness.

3.3 Surface Quality – Contact Profilometer

Surface roughness for each sample was measured using a Mitutoyo Surftest SJ-410 contact profilometer. A vertical column stand was used in combination with a simple toe clamp device to mount each sample manually as shown in Figure 14. The profilometer was set up to automatically eliminate any mounting variation in surface angle. Roughness measurements were collected at a sample height of approximately 26.5mm to correspond

with the thickness measurements collected using the CMM. Measurements were collected on both sides of each sample.

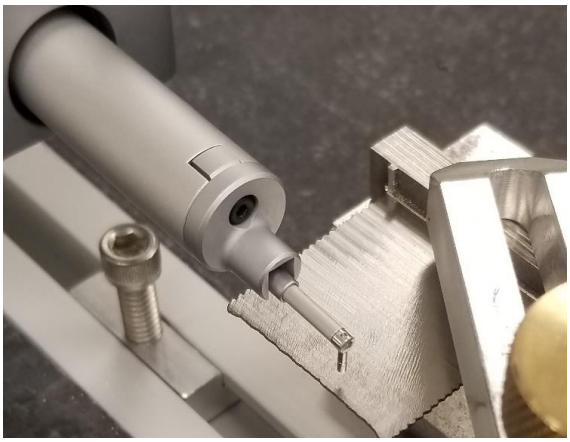

Figure 14: Contact profilometer fixturing setup

For all samples with a wall length of at least 30mm, the primary cut-off wavelength λs value was set as 8μm. This value was used as a maximum cut-off for determining the general shape of the object being measured. The roughness cut-off λc was set as 0.8mm. This value was used to determine the maximum cut-off for data points collected when calculating surface roughness. It was also used as the travel distance for each roughness sample. A sample size of 10 was used resulting in a measurement path that was 8mm in length. This path was manually set to have a midpoint at the center of each sample. A Gaussian filter was used to process the collected data and results are reported in Ra for comparability to external sources. For the samples with a wall length of 10mm, the λc value was changed to 0.25mm and 15 samples were taken resulting in a path length of 3.75mm to avoid collecting data from areas where the supports were connected due to the large radial depth of cut experienced there.

CHAPTER 4. RESULTS AND DISCUSSION

This chapter will provide the results found to evaluate the effect of different support structure parameters on the geometry and roughness of machined thin walls. The first section will compare the results of an unsupported wall to those of an average supported wall to observe the overall impact of adding sacrificial support structures to thin walls. Next, each of the samples with varying geometries tested will be presented with data on geometry and surface roughness to compare the changes between parameters. A brief experimental study on the potential influence of rubbing on the results will be presented. Finally, the time required and quality achieved for each sample will be compared to provide results from the perspective of the inputs required to achieve them.

4.1 Evaluation of Support Structures Relative to Unsupported Case

Comparisons between the unsupported and supported cases showed the largest change in values during the experiment. For these comparisons, both the supported and unsupported walls were 30mm in length (S) and 30mm in height (H). The supported walls used $\alpha=65°$ supports which was the midpoint of the selected angle parameter range and wall length range. All samples were machined to an expected thickness of T=0.5mm. Three samples were produced for each case, and their range of values is represented as error bars. All thicknesses are measured at a height of 26.5mm. Across all samples the error and surface finished improved as height decreased, so this height is meant to serve as a worst-case result based on the highest point that could be measured using the CMM. The plotted value represents the average of the three samples for each parameter set.

4.1.1 Geometric Comparison

The unsupported thin walls showed the highest geometric error during the experiment which corresponds to experiencing the highest deflection during machining. Large amounts of chatter were also present in the unsupported case. Figure 15 shows the comparison between these two sets of samples.

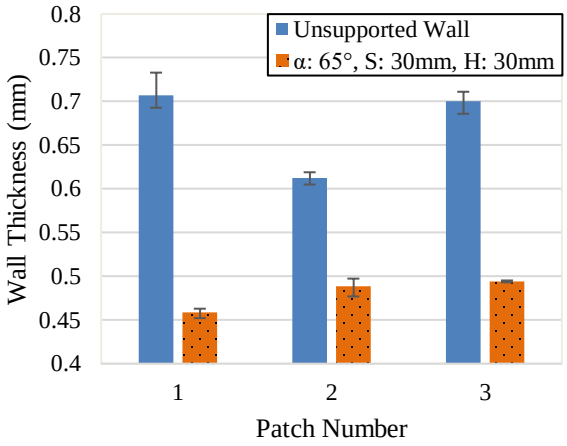

Figure 15: Unsupported thin wall geometric comparison to α=65° supported thin wall at CMM patch locations 1, 2, and 3

The unsupported samples were roughly 0.1-0.2mm oversized after machining while the supported samples were undersized by up to 0.05mm. This geometric error is similar in scale to other investigations of thin wall machining for walls of similar size [42, 45]. For a thin wall with an aspect ratio of 25:1, even higher levels of geometric error have been observed [44]. Variation in geometry size was also more consistent on the supported walls with the largest deviation from the average being 0.012mm versus the largest deviation in the unsupported case which was 0.026mm. Trends can be noted about the geometry across the length of the wall as well. In the unsupported case, each end of the wall was measured to have approximately 0.1mm higher error than the center of the wall. This is due to the

wall bending in multiple directions at the ends of the wall where there was higher stiffness on one side of the point along the wall being machines than on the opposite side. Meanwhile, at the center of the wall there was equal material on both sides of the force being applied resulting in what is approximately 2D bending. In the supported case there was asymmetry in the results where the thickness at Patch 1 was smaller than at Patch 2 and 3. This is likely due to asymmetry in the tool path used. During machining, the end mill traveled in the direction from Patch 1 to Patch 3. As a result, the end mill first contacted the remaining support material at the support nearest to Patch 1 and then eventually encountered the thin wall itself. However, at Patch 3 the end mill was already in contact with the thin wall when it comes into contact with the remaining support material. This increased the radial depth of cut and the cutting forces applied which increases deflection and geometric error at Patch 3. The Patch 2 point exhibited deflection as it was the least supported point along the length of the wall. Asymmetry in the wall thickness across the path being machined was also seen in the thin walls produced by Isaev et al [42] and is attributed to the decrease in wall thickness during machining.

4.1.2 Surface Comparison

Figure 16 compares the surface roughness of the unsupported and 65° supported samples. Two comparisons are shown in the plot to represent the surface roughness on each side of the wall. This is done to illustrate that there is a significant difference in surface quality between the first and second thin wall machining pass for each machining step down, and is represented as Side A and Side B. Columns labelled A represent the surface finish for the side of the wall that was machined first for each A_d=2mm step down during

machining. Similar, columns labelled B show the surface roughness for the side that was machined second for each step down.

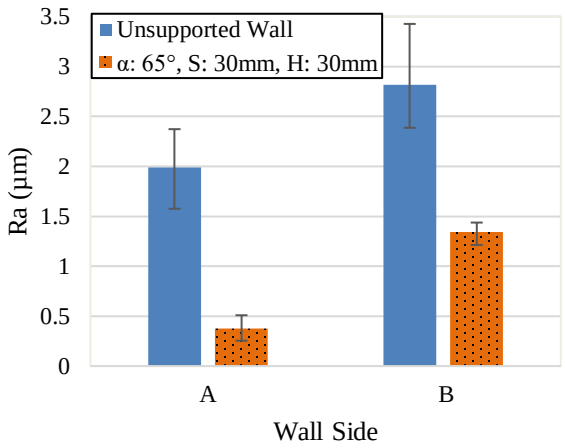

Figure 16: Unsupported thin wall roughness comparison to α=65° supported thin wall measured at a height of 27mm and centered along length of wall, separated by Side A and Side B of each sample

With the machining path used, the first machining pass for each step down (Side A) was performed while the support structure on the opposite side of the thin wall was still intact. This means that the first machining pass has 2mm of additional support that is not present when machining Side B. As a result, the roughness measured on the side of the wall that experienced the first machining path was much lower than the opposite side. Variation between sides in the unsupported case was due to the decreased thickness in the thin wall resulting in higher deflection. Overall, the supported wall surface roughness was approximately 1.5µm lower than the unsupported samples on both sides. Larger error in the unsupported case was much higher due to much larger influence from chatter on the surface finish. The results for Side A were similar to those found in [43] for a wall of similar thickness and height during machining. Although this experiment involved a curved wall which should improve stiffness of the straight walls produced here. The surface

roughness measured on Side B for both samples was high compared to other results found for thicker thin walls [46]. Although higher surface roughness measurements have also been noted for high speed milling of aluminum thin walls [47].

4.2 Evaluation of Changing Support Angle

Samples with supports angles of α=45°, 65°, and 85° were compared to determine the support angle effect on thin wall geometry and surface roughness. Based on the results from the CMM measurement plan, the results were split into 3 different lines. Each line represents the thickness measured for Patch location 1, 2, and 3. The trend for the impact of different support angles is similar, but the overall size varies depending on position.

4.2.1 Geometric Comparison

All samples used for support angle comparison showed similar trends across the length of the wall to the baseline α=65° support wall used for the unsupported comparison. The wall was thinner where the end mill first contacted the wall, and similar thickness measurements were seen at the Patch 2 and Patch 3 points. All three of these points are plotted below to show their differences and to serve as additional points for validation of the influence of different support angles.

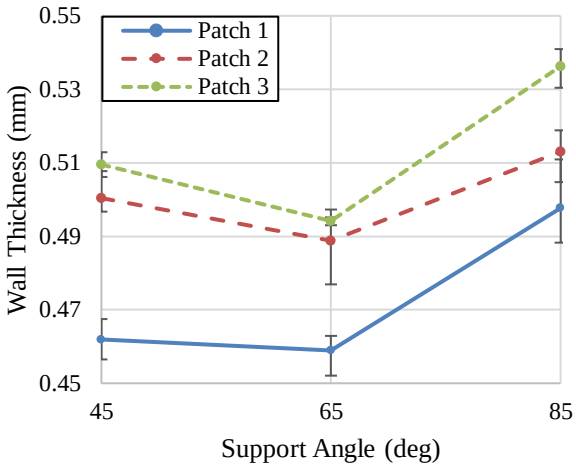

Figure 17: Influence of support angle (α) on wall thickness measured at CMM patch location 1, 2, and 3

As seen in Figure 17, wall thickness increased between α=65° and α=85° as would be expected as the support structure was less substantial, this allowing an increase in wall deflection during machining. Between α=45° and α=65° the thickness appeared to decrease slightly. This change is close to placing within the error bars generated based on the spread of 3 samples, however this discrepancy could also be due to the order in which the samples were produced. The α=65° supported wall samples were the first samples to be produced with an unused tool. Meanwhile the α=45° were produced near the end of all the samples made. Tool wear may have been an influence on these results as the sharpness of the tool can greatly impact the cutting forces applied to the thin wall and therefore increase wall deflection and thickness [41]. The use of a sharper tool on the α=65° samples may have resulted in lower wall thickness for those samples compared to samples produced after the end mill had been used several times. Overall change in wall thickness between α=45° supports and α=85° supports was roughly 0.02mm. The cost of this improvement in geometry is relatively high as significantly more printing and machining time was required for the α=45° support. This will be explored further in Section 4.6.

4.2.2 Surface Comparison

The surface finish on supported walls changed at a much larger scale as the support angle was varied. Figure 18 shows these results for each side of the wall listed as Side A and Side B. Side A represents the machining pass where the supports on the opposite side of the wall were still present when machining the thin wall, and on Side B the supports on the opposite side of the wall have already been machined, and was therefore less stiff. Error bars are represented by the range of values measured for the three samples at each support angle.

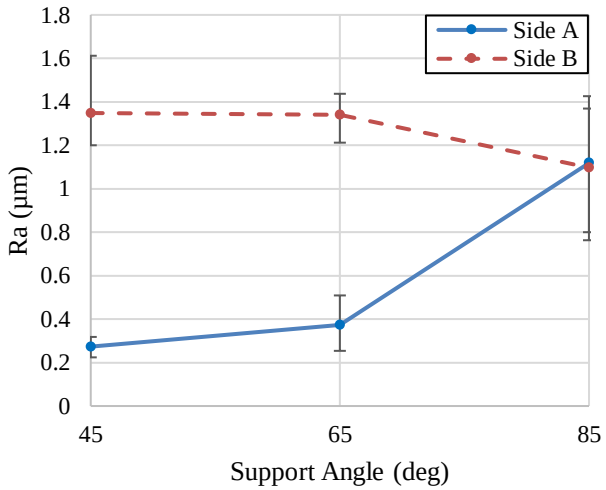

Figure 18: Effect of support angle (α) on surface roughness measured at a height of 27mm and centered along length of thin wall, separated by Side A and Side B of each sample

The surface roughness measured for Side A see an exponential increase in surface roughness as support angle was increased. By α=85° the surface finish on Side A of the wall was similar to the surface finish seen on Side B of the wall. At α=45° and α=65°, the surface roughness was extremely low and near the limit for surface finishes reasonably obtainable through milling. Side B of the thin wall remained relatively unchanged as support angles changed but was still significantly improved over the unsupported case.

This was again due to the removal of the supports on the opposing side of the thin wall, resulting in a decrease in stiffness during the machining of Side B. However, the overall surface roughness of Side B was still much higher than Side A for most support angles. At α=85° the surface roughness also varied much more widely, this was likely due to increased chatter on the surface that could have influenced the results.

4.3 Evaluation of Changing Support Spacing

To evaluate the impact of different support spacing schemes, three samples were produced for each wall length of S=10mm, 30mm, and 50mm. The support angle was fixed at α=65°, and the support was printed to the full height of the thin wall. The results are shown in Figure 18 below. Due to the length of the 10mm sample, results are only shown for the center of each wall for the S=10mm sample as there was insufficient space along the length of the 10mm sample to collect thickness measurements at multiple points.

4.3.1 Geometric Comparison

The results shown in Figure 19 are generally as expected for the S=30mm and S=50mm support spacing samples. Deflection increased as the supports were spaced further apart. The center and end of Side B had similar geometries as in the previous samples. The end of the Side A wall had smaller thickness due to smaller machining forces from lower radial depth of cut. The scale of the change between S=30mm and S=50mm was approximately 0.04mm which is double the change seen between the α=45° and α=85° support angle changes.

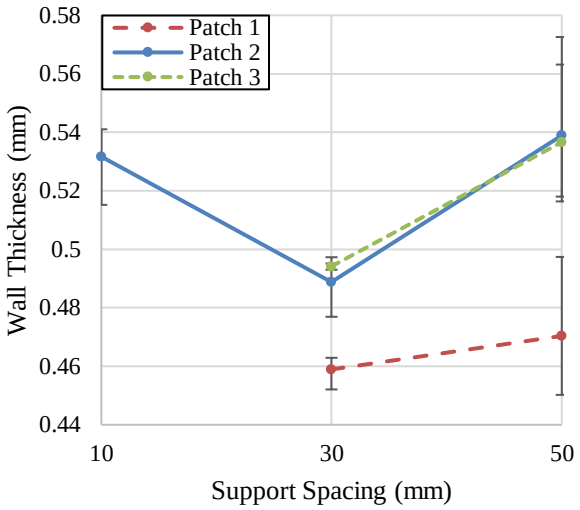

Figure 19: Influence of support spacing (S) on wall thickness measured at CMM patch locations 1, 2, and 3

The S=10mm sample was thicker than the 30mm support spacing and was roughly similar to the 50mm support spacing samples. This result was likely due to unintended loss in stiffness from the decreased length of the wall rather than the change in support spacing. Decreasing the support spacing between S=30mm and S=10mm would have been expected to reduce the deflection experienced during machining. Therefore, this result was likely more representative of the impact of length of the wall itself on deflection rather than support spacing. If a standalone thin wall were to be machined the length of the thin wall would influence the deflection experienced. A longer wall would deflect less and have lower geometric error than a shorter wall. Additionally, Figure 20 below shows a sample of the scan data collected using the CMM. A rapid change in thickness across a given height of the thin wall can be seen. This rapid change may have resulted in error when fitting accurate planes to the surface of the thin wall.

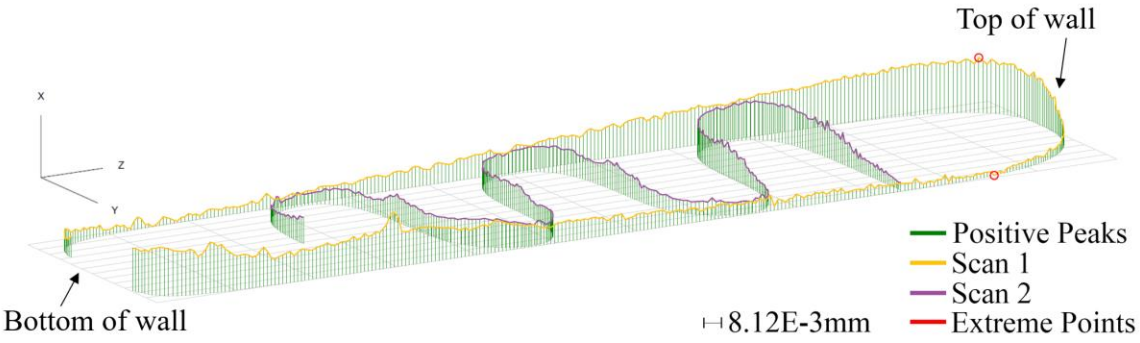

Figure 20: Raw CMM point data for side A of a 10mm thin wall sample showing poor flatness along top length of wall by circled extreme points and large variation in X direction

4.3.2 Surface Comparison

Despite the unintended deflection present in the S=10mm sample for geometric comparison, the surface roughness measured on the samples appear to plot as expected. Support spacing was the only parameter tested that appeared to influence the surface roughness for Side B of supported walls. Figure 21 shows that both Side A and Side B of the wall improved in surface roughness as support spacing was decreased. Increasing the density of support structures was expected to improve the stiffness of the workpiece overall which reduces the potential for chatter during machining. The improvement of surface roughness on Side B suggests that surfaces in closer proximity to the support structure will have a lower surface roughness on both sides of the wall. The stiffness provided by the support structure may rapidly decay for Side B at surface locations further away from the support structure. This is evident by the contact profilometer location for all other samples being located further away from the support structures, and correspondingly all other samples exhibiting higher surface roughness values.

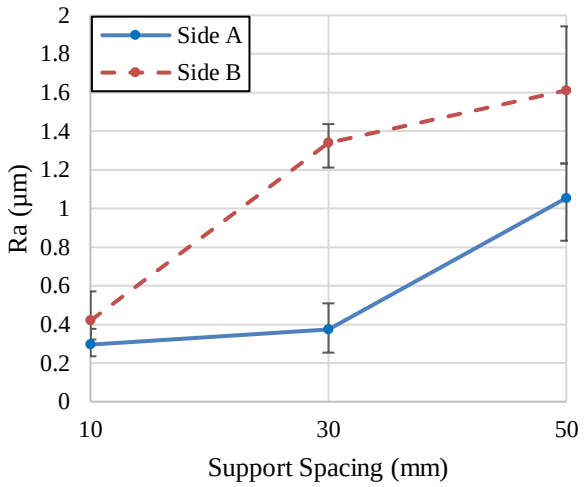

Figure 21: Effect of support spacing (S) on surface roughness measured at a height of 27mm and centered along length of thin wall, separated by Side A and Side B of each sample

For the Side A of the wall the surface roughness for support spacing corresponded to values similar to changing support angle. At S=10mm support spacing the surface finish was at the low end of what can be expected from milling, and at S=50mm the surface showed some evidence of chatter and increased surface roughness. There was only a small increase in surface roughness between S=10mm and S=30mm spacing, although this would represent a major increase in material used and printing and machining time required. For Side B of the wall however, there was a very large increase in surface roughness between S=10mm and S=30mm. Surface roughness for the S=10mm sample was the lowest Side B roughness measured for all parameters. However, this would appear to be opposite what might be expected when compared to the geometric error that was present on the S=10mm samples. This result may indicate that surface roughness and geometric error are not necessarily coupled due to the influence of chatter. The S=10mm sample may have had high deflection due to its short length, but the geometry avoided any chatter and therefore enabled a low surface roughness.

4.4 Evaluation of Changing Support Height

As with the other two parameters, height was evaluated at three different levels: H=10mm, 20mm, and 30mm. Three samples were evaluated for each height level. The support angle for all of the samples was fixed at α=65°. The height parameter displayed the largest range of thicknesses of the three tested parameters. Results are again shown separated by position along the length of the wall. Although the samples with H=10mm support heights had the highest deflection, they performed noticeably better than the unsupported case for a relatively small print time and material addition.

4.4.1 Geometric Comparison

The support height samples performed largely as expected when measured for geometric error. An exponential change in wall thickness was expected with changing support height when compared to a simple beam deflection equation. However, increasing support height resulted in an almost linear decrease in wall thickness as shown in Figure 22. Overall difference between the H=10mm support height and 30mm support height was approximately 0.08mm. The H=10mm support height samples showed an unexpected change in geometry between the H=20mm and H=10mm support heights where the geometry remained relatively consistent at the center of the thin wall but continued to increase in thickness as support height decreased at the both ends of the wall. This result was comparable to the geometry found on unsupported samples suggesting that at 10mm support heights the ends of the wall are no longer stiffer than the center of the wall. This allows for the ends of the walls to deflect more than the center of the wall as was the case

in the unsupported samples. Conversely, supported samples tended to deflect more in the center as the ends of the walls were stiffer.

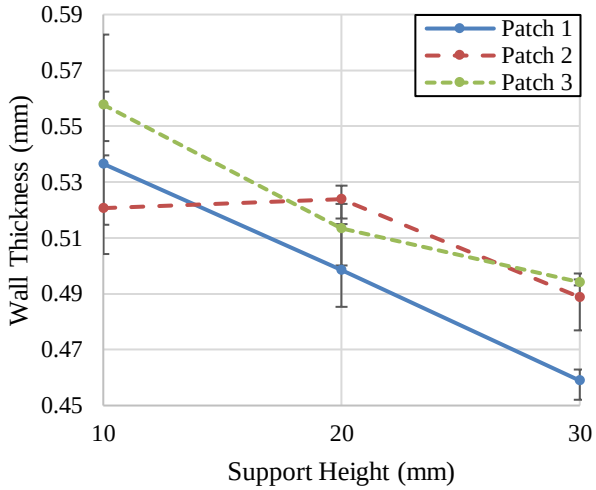

Figure 22: Influence of support height (H) on wall thickness measured at CMM patch locations 1, 2, and 3

4.4.2 Surface Comparison

The surface roughness for Side A of machining when varying support height also decreased relatively linearly as support height increased. Figure 23 shows that despite the effective reduction in deflection that the H=20mm supports provided, the surface roughness for the H=10mm and H=20mm support heights were similar for both machining passes. At a roughness of around 1.5µm this finish was on the high side of measured values. It was not until the support reached to the full height of the wall that Side A was measured to have a lower surface roughness than Side B. Side B surface roughness remained relatively consistent regardless of the support height chosen. The support height samples were also the only samples to produce potentially higher surface roughness on Side A than Side B. Although the difference between the two sides was within the margin of error for H=10mm. Since the location for measuring surface roughness was above the H=20mm

height point, both sides of the wall lacked support material on their respective opposing sides which resulted in similar surface roughness results on both sides for the H=10mm and H=20mm samples.

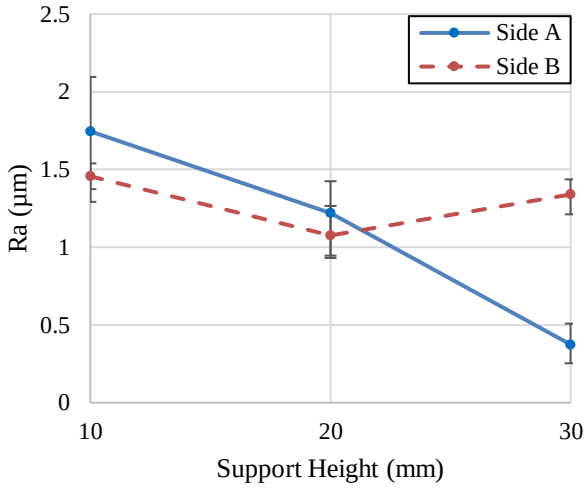

Figure 23: Effect of support height (H) on surface roughness measured at a height of 27mm and centered along length of thin wall, separated by Side A and Side B of each sample

Although the surface roughness appeared to decrease slightly between support heights of H=10mm and H=20mm, this was likely measurement error due to the influence of chatter and a larger sample size would likely show relatively constant values between these two support heights. Chatter was visually apparent on the surface of both of these samples. Based on these results, and the results from the other parameters tested, the surface roughness of Side B appears to be generally the same regardless of support shape and only depends on the proximity of the support itself.

4.5 Effect of Tool Rubbing on Results

As mentioned previously, the use of a tool with a flute length that was longer than the axial depth of cut influenced the scale of the results presented. As machining forces

caused deflection and therefore geometric error in the machined thin wall this resulted in geometry along the wall that would still remain within reach of the endmill along the designed toolpath. Subsequent step downs would continue to re-machine previous steps resulting in a final geometry that was thinner than would have resulted from a single isolated machining path for each A_d=2mm step down path. To quantify this effect, an experiment was performed on an unsupported this wall where a region at the top of the wall was measured using a micrometer after each step down. The results of this experiment are shown in Figure 24.

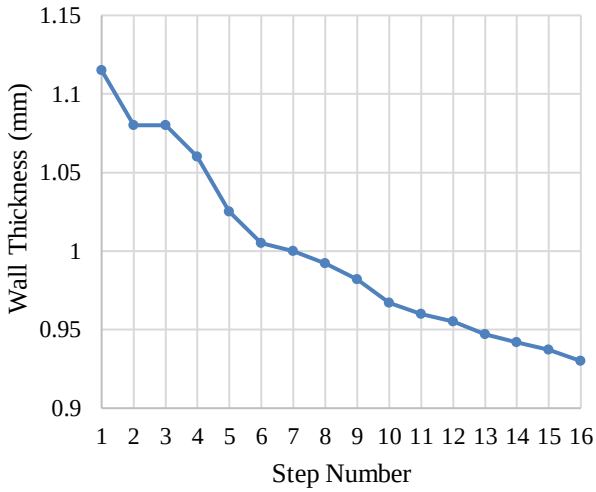

Figure 24: Change in wall thickness measured after each A_d=2mm step-down machining pass at a single point located at the top of an unsupported thin wall

These results show slightly under 0.2mm of material removed between the first and final pass for the thin wall. This effect was expected to be largest at the top of the thin wall and then decrease to a flat line at the bottom of the wall where negligible deflection was expected. As the results shown for the three changing parameters were all compared based on specific points near the top of the wall, the trends of the results were expected to remain the same with the final geometry scaling based on the number of passes used to machine

the wall. The rubbing of the endmill on previous step downs was also likely the cause for some samples showing geometry that was smaller than the expected geometry. The deflection experienced by the thin wall acts in some degree to cause the thin wall to both move away from the endmill and move back towards the endmill which allows for additional material to be removed beyond the dimensions expected from the 0.5mm designed tool path. Therefore, when producing thin walls, the effect of rubbing can considerably alter the final geometry of the thin wall and should be accounted for if the flute length of the end mill is longer than the axial depth of cut used for each step down.

4.6 Comparison of Estimated Production Times for Support Schemes

After observing the effect of different sacrificial support parameters on the final quality of thin walls, comparisons are made to see the relationship between support angle, height, and spacing relative to the print time required to produce each support scheme. To produce these results, the toolpaths used to produce each sacrificial support sample were summed and multiplied by the feed rate used during deposition to determine an approximate print time. This method neglects rapid moves of the machine between each bead. However, this was a negligible difference relative to the feed moves. As the same basic tool path was used for each support samples with only the length of beads changing, the rapid moves would also be similar for all tool paths with the exception of the unsupported case. Machining time was also not included in these parameters. The machining tool paths used in the parameter test experiments varied directly with the additive tool paths, and so did not change the comparison of time required relative to quality of thin walls produced. To compare the print time for samples with varying wall lengths compensations were applied to the S=10mm and S=50mm support spacing print

times to make these support schemes comparable to the S=30mm wall samples. The S=10mm support spacing print time was increased to represent a S=30mm wall with 4 supports along each side of its length. The S=50mm sample was multiplied by 0.6 to represent that this support scheme would only require 60% of the sacrificial supports compared to a wall that had S=30mm support spacing. Figure 25 presents all the tested samples relative to their respective print times and the finished wall thickness. The plotted values are an average across the length of the wall as well as across the three samples produced for each support parameter.

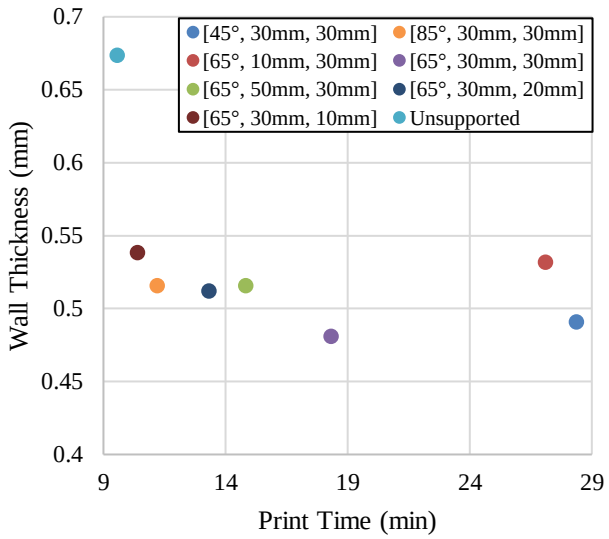

Figure 25: Comparison of average final geometry relative to print time for all parameters [α, S, H] representing support angle, support spacing, and support height respectively

This figure illustrates that there was relatively little improvement in final wall geometry after around 11 minutes corresponding to the α=85° sacrificial supports. The α=65° and α=45° supports both achieved a lower wall thickness but took 2-3 times longer to print. The S=10mm support spacing geometry results are represented the same as they were in Section 4.3.1 which means that the unintended influence of the short wall length causing an increasing in deflection was still present. In a scenario where the S=10mm

support spacing was implemented on a thin wall with a longer length the wall deflection would be lower, and the value of the additional print time required would be better represented.

Next, Figure 26 and 27 show the comparison between print time required to produce a sample and the corresponding Ra value achieved after machining. Results are presented with the same print time compensations for the S=10mm and S=50mm support spacing samples. Values presented are an average of the three samples produced for each support parameter.

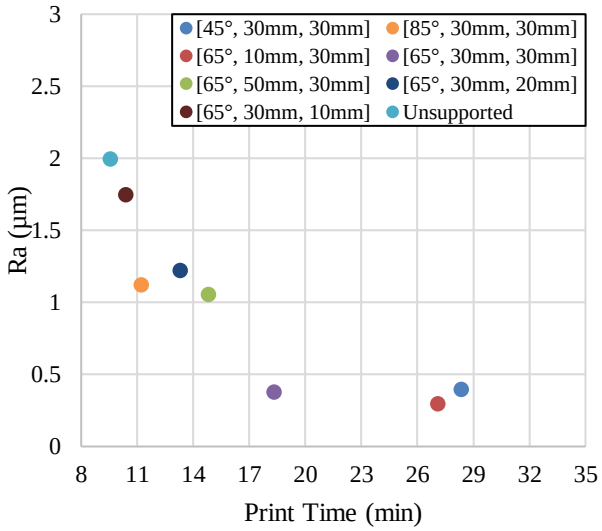

Figure 26: Comparison of average surface roughness on Side A relative to print time for all parameters [α, S, H] representing support angle, support spacing, and support height respectively

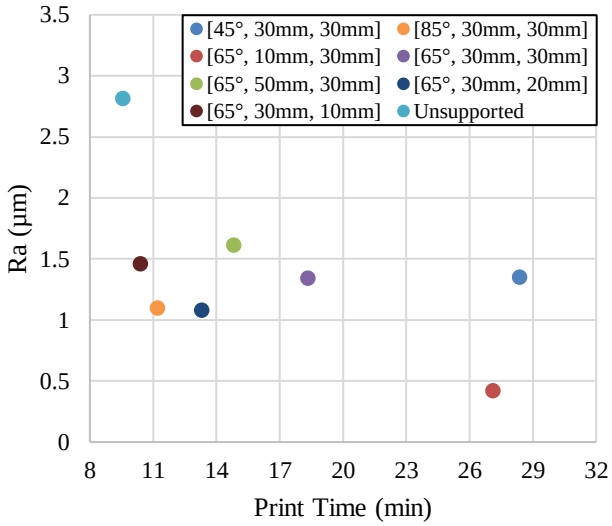

Figure 27: Comparison of average surface roughness on Side B relative to print time for all parameters [α, S, H] representing support angle, support spacing, and support height respectively

For Side A surface roughness, support schemes that required longer print times generally enabled a lower surface roughness. Although the S=10mm support spacing and α=45° support angle do not appear to provide a significant improvement of the α=65° support angle for Side A machining. The H=10mm support height samples required the least time to produce but showed little improvement in surface roughness. The α=45° support angle samples required the longest print time and showed the largest decrease in geometric error, but still did not improve the surface roughness on Side B. The S=10mm support spacing was the only sample that appears to improve surface finish in an appreciable amount. The α=85° support angle and H=20mm support height samples appeared to provide a small decrease in surface roughness, but it is likely that this was due to the sample size and a larger sample size would show results similar to most other support schemes.

CHAPTER 5. CONCLUSION

This chapter will summarize the results from the experiments performed and review the conclusions that can be drawn from these results. Limitations of this work as well as possible subjects for future work will also be discussed.

5.1 Conclusions

This work presents a novel method of improving the geometric accuracy and surface finish of high aspect ratio thin walls produced using a hybrid manufacturing combination of blown powder direct energy deposition and CNC machining. Adding simple sacrificial support structures onto a thin wall feature at regular intervals can enable an effective reduction in the deflection experienced during finish machining. The work shown in this paper illustrates how the angle, spacing, and height of this support can be varied to meet the tolerance needs of a specific feature. The addition of any type of sacrificial support structure can quickly allow for a tighter tolerance thin wall, further increasing the stiffness of the support appears to have rapidly diminishing effects but can nonetheless be used to allow for even higher thin wall quality.

Adding the least substantial supports at each end of a thin wall with an angle of $\alpha=85°$ enabled an average reduction in geometric error of 0.16mm. Increasing the support angle to $\alpha=45°$ increases this to 0.18mm. However, the $\alpha=45°$ supports required nearly 3 times the print time compared to the unsupported case. For surface finish the sacrificial supports provided between a reduction in surface roughness between 0.89µm and 1.71µm for $\alpha=85°$ and $\alpha=45°$ supports respectively for Side A of these samples. For Side B of the

wall the machined the surface roughness was reduced by around 1.47µm but did not significantly vary between different support angles. Changing the distance between each support enabled a deflection reduction between 0.16µm and 0.19µm for S=50mm and S=30mm support spacing. Unintended influences on the experiment leave the S=10mm support spacing inconclusive. Changing support spacing was the only parameter tested that appeared to influence the surface roughness measured for Side B. At S=10mm Side B surface roughness was reduced by 1.76µm. Side A of the wall saw similar roughness reductions. The support height parameter saw roughly linear reductions in geometric error as the height increased. Geometric error was reduced between 0.13mm and 0.19mm. Surface roughness was reduced by a maximum of 1.626µm with full support height for Side A, but again saw an average reduction in surface roughness of 1.52µm on Side B with no major variation for changing support height. Comparisons of geometric error and surface roughness to print time were also presented. For deflection, only marginal gains were seen for support schemes that took longer than roughly 11 minutes to print which corresponded to the α=85° sacrificial supports. Surface roughness on Side A of the samples did see significant reductions as print time increased up to the α=65° supports which required 18.3 minutes to print. For Side B there was no major differences between support schemes except for the 10mm support spacing samples which had the second longest print time at 27.1 minutes.

5.2 Limitations and Future Work

Several limitations were present in the presented work above that leave possibilities for future experiments to further explore the use of sacrificial support structures in hybrid thin wall manufacturing. The first limitation was the assumption on the relation between

thin wall geometry and deflection. Section 4.5 covers on example of error in this assumption, machining samples while avoiding re-machining may provide further understanding of these support structures. Additionally, experiments that could measure deflection during machining directly would assist in eliminating unwanted influences on the effect of different support parameters. Future works might also study the benefits on different tool paths. The high surface roughness present on Side B of each sample could likely be alleviated through alternate machining paths. Finally, investigations into the use of support structures with more complex geometries such as overhangs were not feasible with the tested printing capabilities on the machine used for this work, but may allow additional reductions in printing and machining times without a large decrease in effectiveness.

APPENDIX A. CMM AND PROFILOMETER EXAMPLE DATA

A.1 Example Coordinate Measuring Machine Raw Data

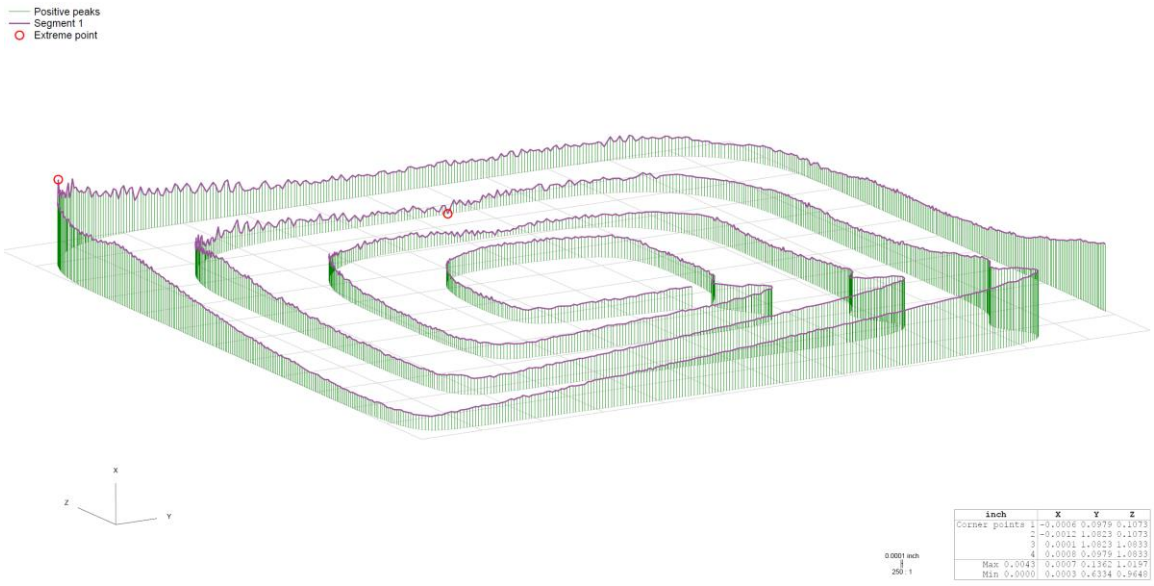

Figure A1: 65° support angle, 30mm length, 30mm height CMM scan data

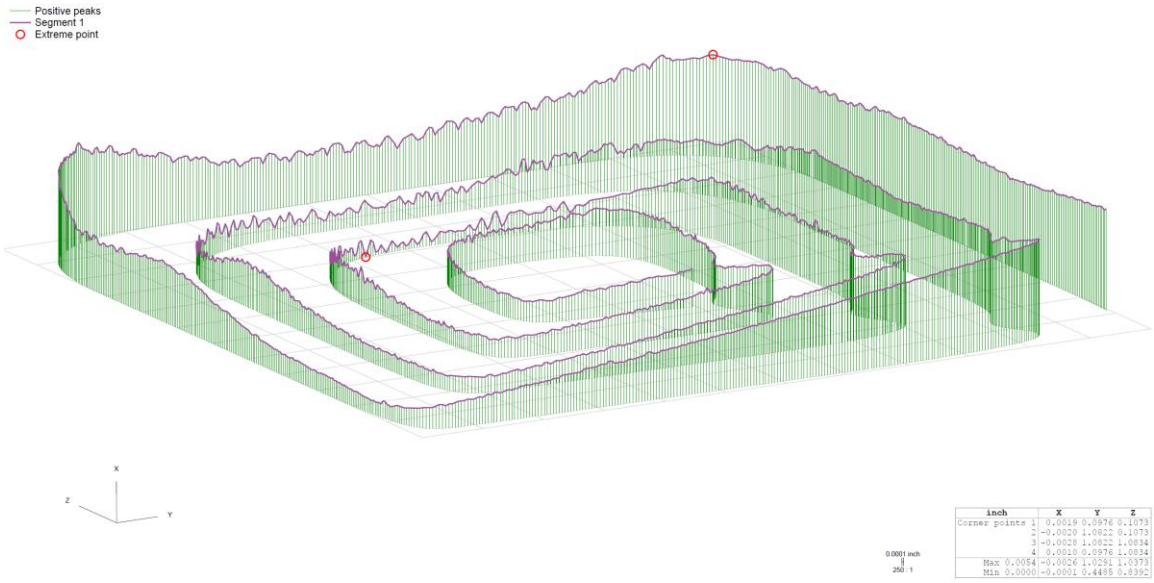

Figure A2: Unsupported thin wall CMM scan data

A.2 Example Contact Profilometer Raw Data

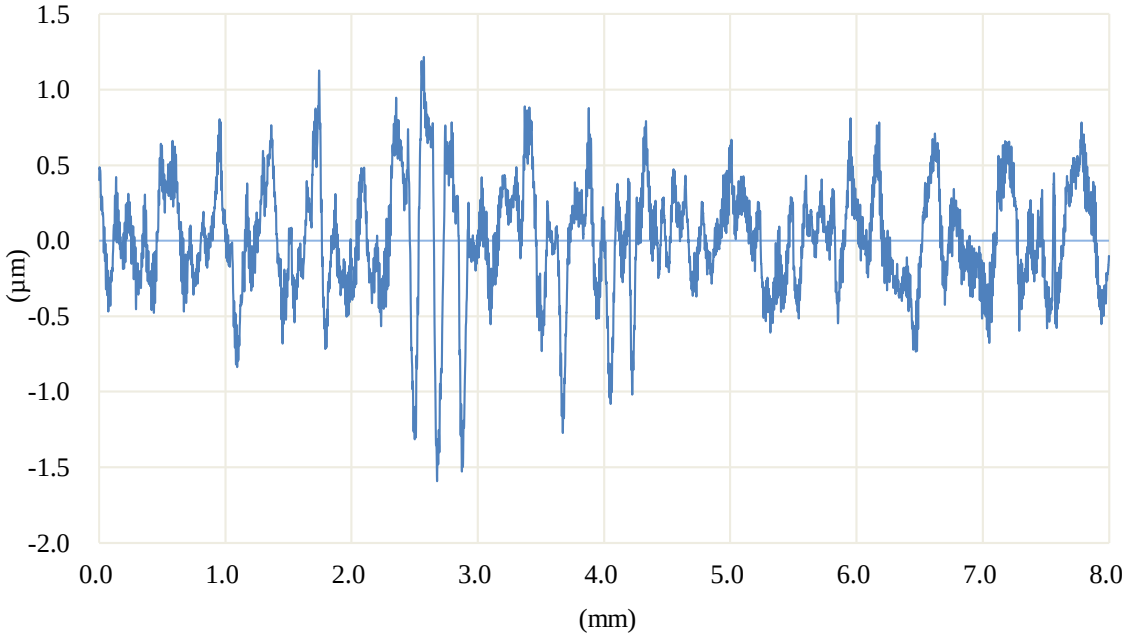

Figure A3: Contact profilometer raw data for 65° support angle, 30mm length, 30mm height sample

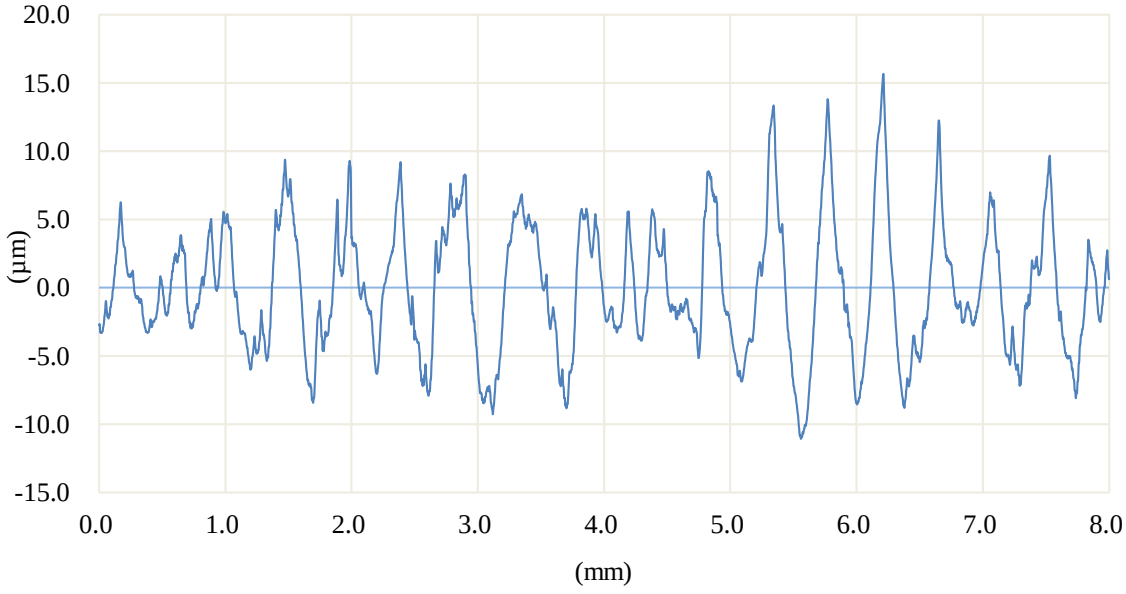

Figure A4: Contact profilometer raw data for unsupported thin wall

REFERENCES

[1] Donoghue J, Antonysamy AA, Martina F, et al. The effectiveness of combining rolling deformation with wire-arc additive manufacture onβ-grain refinement and texture modification in Ti-6Al-4V. Mater Charact[Internet].2016;114:103–114.

[2] Williams SW, Martina F, Addison AC, et al. Wire+Arc additive manufacturing. Mater Sci Technol [Internet].2016;32(7):641–647.

[3] Shim, Do-Sik, Gyeong-Yun Baek, and Eun-Mi Lee. "Effect of substrate preheating by induction heater on direct energy deposition of AISI M4 powder." *Materials Science and Engineering: A* 682 (2017): 550-562.

[4] Zhang, Yongzhong Z., Chris Meacock, and Rui Vilar. "Laser powder micro-deposition of compositional gradient Ti–Cr alloy." *Materials & Design* 31.8 (2010): 3891-3895.

[5] Brueckner, Frank, et al. "Process characteristics in high-precision laser metal deposition using wire and powder." *Journal of Laser Applications* 29.2 (2017): 022301.

[6] Herranz, S., et al. "The milling of airframe components with low rigidity: a general approach to avoid static and dynamic problems." *Proceedings of the Institution of Mechanical Engineers, Part B: Journal of Engineering Manufacture* 219.11 (2005): 789-801.

[7] Tlusty, J., S. Smith, and W. R. Winfough. "Techniques for the use of long slender end mills in high-speed milling." *CIRP annals* 45.1 (1996): 393-396.

[8] Li, Bao-Qiang, et al. "Research on surface roughness of AlSi10Mg parts fabricated by laser powder bed fusion." *Metals* 8.7 (2018): 524.

[9] Patel, Sagar, Allan Rogalsky, and Mihaela Vlasea. "Towards understanding side-skin surface characteristics in laser powder bed fusion." *Journal of Materials Research* 35.15 (2020): 2055-2064.

[10] Xiong, Jun, et al. "Influences of process parameters on surface roughness of multi-layer single-pass thin-walled parts in GMAW-based additive manufacturing." *Journal of Materials Processing Technology* 252 (2018): 128-136.

[11] Srinivasan, Harshad, Ola LA Harrysson, and Richard A. Wysk. "Automatic part localization in a CNC machine coordinate system by means of 3D scans." *The International Journal of Advanced Manufacturing Technology* 81.5-8 (2015): 1127-1138.

[12] Yamazaki, Taku. "Development of a hybrid multi-tasking machine tool: integration of additive manufacturing technology with CNC machining." *Procedia Cirp* 42 (2016): 81-86.

[13] "LASERTEC 65 DED hybrid." *DMG Mori*, https://us.dmgmori.com/products/machines/additive-manufacturing/powder-nozzle/lasertec-65-ded-hybrid. Accessed 18 October 2020.

[14] Lorenz, K. A., et al. "A review of hybrid manufacturing." *Solid freeform fabrication conference proceedings*. Vol. 53. 2015.

[15] "MPA - A MPA Powder Application Technique." *Hermle*, https://www.hermle.de/en/services/additive_manufacturing/technology_mpa. Accessed 9 October 2020.

[16] Gibson, B. T., et al. "Melt pool size control through multiple closed-loop modalities in laser-wire directed energy deposition of Ti-6Al-4V." *Additive Manufacturing* 32 (2020): 100993.

[17] Amine, Tarak, Joseph W. Newkirk, and Frank Liou. "An investigation of the effect of laser deposition parameters on characteristics of multilayered 316 L deposits." *The International Journal of Advanced Manufacturing Technology* 73.9-12 (2014): 1739-1749.

[18] Mukherjee, T., and Tarasankar DebRoy. "Printability of 316 stainless steel." *Science and Technology of Welding and Joining* 24.5 (2019): 412-419.

[19] Beese, Allison M., and Beth E. Carroll. "Review of mechanical properties of Ti-6Al-4V made by laser-based additive manufacturing using powder feedstock." *Jom* 68.3 (2016): 724-734.

[20] "LUMEX Avance-25." *Lumex Matsuura*, https://www.lumex-matsuura.com/english/LUMEX-Avance-25. Accessed 13 October 2020.

[21] Bałon, Paweł, et al. "Implementation of high speed machining in thin-walled aircraft integral elements." *Open Engineering* 8.1 (2018): 162-169.

[22] Smith, S., and D. Dvorak. "Tool path strategies for high speed milling aluminum workpieces with thin webs." *Mechatronics* 8.4 (1998): 291-300.

[23] Tlusty, Jiri. "High-speed machining." *CIRP annals* 42.2 (1993): 733-738.

[24] Bravo, U., et al. "Stability limits of milling considering the flexibility of the workpiece and the machine." *International Journal of machine tools and manufacture* 45.15 (2005): 1669-1680.

[25] Bolar, Gururaj, and Shrikrishna N. Joshi. "Numerical Modeling and Experimental Validation of Machining of Low-Rigidity Thin-Wall Parts." *Precision Product-Process Design and Optimization*. Springer, Singapore, 2018. 99-122.

[26] Tang, Aijun, and Zhanqiang Liu. "Three-dimensional stability lobe and maximum material removal rate in end milling of thin-walled plate." *The International Journal of Advanced Manufacturing Technology* 43.1-2 (2009): 33-39.

[27] Wu, Qiong, Da-Peng Li, and Yi-Du Zhang. "Detecting milling deformation in 7075 aluminum alloy aeronautical monolithic components using the quasi-symmetric machining method." *Metals* 6.4 (2016): 80.

[28] Wang, Jun, Soichi Ibaraki, and Atsushi Matsubara. "A cutting sequence optimization algorithm to reduce the workpiece deformation in thin-wall machining." *Precision Engineering* 50 (2017): 506-514.

[29] Koike, Yusuke, Atsushi Matsubara, and Iwao Yamaji. "Optimization of cutting path for minimizing workpiece displacement at the cutting point: changing the material removal process, feed direction, and tool orientation." *Procedia CIRP* 5 (2013): 31-36.

[30] Ratchev, Svetan, et al. "Milling error prediction and compensation in machining of low-rigidity parts." *International Journal of Machine Tools and Manufacture* 44.15 (2004): 1629-1641.

[31] Ratchev, S., S. Liu, and A. A. Becker. "Error compensation strategy in milling flexible thin-wall parts." *Journal of Materials Processing Technology* 162 (2005): 673-681.

[32] Budak, Erhan, et al. "Prediction of workpiece dynamics and its effects on chatter stability in milling." *CIRP annals* 61.1 (2012): 339-342.

[33] Tang, Aijun, and Zhanqiang Liu. "Three-dimensional stability lobe and maximum material removal rate in end milling of thin-walled plate." *The International Journal of Advanced Manufacturing Technology* 43.1-2 (2009): 33-39.

[34] Ge, Guangyan, et al. "An integrated error compensation method based on on-machine measurement for thin web parts machining." *Precision Engineering* (2020).

[35] Smith, Scott, et al. "Sacrificial structure preforms for thin part machining." *CIRP annals* 61.1 (2012): 379-382.

[36] Zeng, Shasha, et al. "A novel approach to fixture design on suppressing machining vibration of flexible workpiece." *International journal of machine tools and manufacture* 58 (2012): 29-43.

[37] Kolluru, Kiran, Dragos Axinte, and Adib Becker. "A solution for minimising vibrations in milling of thin walled casings by applying dampers to workpiece surface." *CIRP Annals* 62.1 (2013): 415-418.

[38] "Rigidax Tooling & Fixturing Wax." *MachineableWax.com*, https://www.machinablewax.com/product.php?product=44. Accessed 9 October 2020.

[39] Kolluru, K., and D. Axinte. "Novel ancillary device for minimising machining vibrations in thin wall assemblies." *International Journal of Machine Tools and Manufacture* 85 (2014): 79-86.

[40] Jiang, Xiaohui, Guokuan Zhao, and Weiwei Lu. "Vibration suppression of complex thin-walled workpiece based on magnetorheological fixture." *The International Journal of Advanced Manufacturing Technology* 106.3-4 (2020): 1043-1055.

[41] Lee, L. C., K. S. Lee, and C. S. Gan. "On the correlation between dynamic cutting force and tool wear." *International Journal of Machine Tools and Manufacture* 29.3 (1989): 295-303.

[42] Alexander, Isaev, et al. "Machining of thin-walled parts produced by additive manufacturing technologies." *Procedia* CIRP 41 (2016): 1023-1026.

[43] Bolar, Gururaj, et al. "Experimental investigation on surface quality and dimensional accuracy during curvilinear thin-wall machining." *Materials Today*: Proceedings 5.2 (2018): 6461-6469.

[44] Izamshah, Raja, et al. "Effects of end mill helix angle on accuracy for machining thin-rib aerospace component." *Applied Mechanics and Materials*. Vol. 315. Trans Tech Publications Ltd, 2013.

[45] Ślusarczyk, Łukasz. "Analysis of deformations of thin wall parts in machining." *Proceedings of SPIE*. Vol. 9662. 2015.

[46] Bolar, G., and S. N. Joshi. "An Experimental Investigation on Productivity and Product Quality During Thin-Wall Machining of Aluminum Alloy 2024-T351." *Advances in Forming, Machining and Automation*. Springer, Singapore, 2019. 385-393.

[47] Seguy, Sébastien, Gilles Dessein, and Lionel Arnaud. "Surface roughness variation of thin wall milling, related to modal interactions." *International Journal of Machine Tools and Manufacture* 48.3-4 (2008): 261-274.